

# Heterogeneous Nucleation onto Ions and Neutralized Ions: Insights into Sign-Preference

Juha Kangasluoma,<sup>\*,†</sup> Alexander Samodurov,<sup>†</sup> Michel Attoui,<sup>†,‡</sup> Alessandro Franchin,<sup>†</sup> Heikki Junninen,<sup>†</sup> Frans Korhonen,<sup>†</sup> Theo Kurtén,<sup>§</sup> Hanna Vehkamäki,<sup>†</sup> Mikko Sipilä,<sup>†</sup> Katrianne Lehtipalo,<sup>†,⊥</sup> Douglas R. Worsnop,<sup>†,||</sup> Tuukka Petäjä,<sup>†</sup> and Markku Kulmala<sup>†</sup>

<sup>†</sup>Department of Physics, University of Helsinki, P.O. Box 64, 00014 Helsinki, Finland

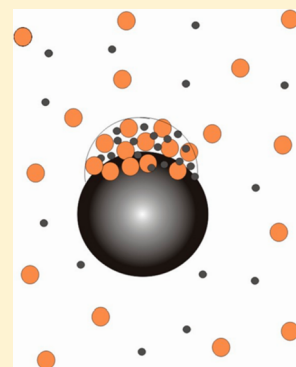
<sup>‡</sup>University Paris Est Creteil, University Paris-Diderot, LISA, UMR CNRS 7583, Paris, France

<sup>§</sup>Department of Chemistry, University of Helsinki, P.O. Box 55, 00014 Helsinki, Finland

<sup>||</sup>Aerodyne Research Inc., Billerica, Massachusetts, United States

<sup>⊥</sup>Paul Scherrer Institut, 5232 Villigen PSI, Switzerland

**ABSTRACT:** Heterogeneous nucleation of vapor on a seed particle surface is dependent on the seed properties such as size, chemical composition, and electric charging state, of which the significance of the charging state has not been uncovered unambiguously. The underlying problem is that, on the molecular level, the charging state and the chemical composition of the seed are connected and cannot be well separated without a direct mass spectrometric measurement of the ion. By generating sub-3 nm size selected seeds of different size, chemical composition, electric charging state, and letting three different vapors nucleate onto the seeds, we show that heterogeneous nucleation does not clearly prefer either positive or negative seeds. Rather, the most important parameter determining the nucleation probability in the sub-3 nm size range was the seed chemical composition. Our findings help to understand the dynamics in various nanoparticle systems, such as nucleation chambers, industrial processes, or atmospheric aerosols.



## INTRODUCTION

Nucleation from gas to liquid or solid phase is an important phase transformation process for example in material sciences, nanomaterial synthesis, and the formation of atmospheric aerosol particles. An energy barrier needs to be overcome before nucleation occurs. In nucleation from gas to solid phase, a seed particle significantly reduces the energy barrier, making heterogeneous nucleation favored over homogeneous nucleation. As found by Wilson<sup>1</sup> already a century ago in pioneering expansion chamber experiments, charged seeds, ions, further mitigate the energy barrier and enhance cloud droplet formation, thus potentially playing an important role in atmospheric cloud formation.<sup>2</sup> Wilson also reported that in a nucleation chamber, at constant water supersaturation, the presence of negative ions induces more fog, or cloud droplets, than the presence of positive ions (negative sign preference). After Wilson's experiments many experimental results have been published on sign preference, with contradicting findings. Negative sign preference for ion-induced nucleation has been found, e.g., in refs 3–5, positive preference, e.g., in refs 6–9, no preference in ref 10, and a system specific preference in refs 11 and 12. Much of the controversy can be due to uncertainty in the chemical composition of the ions, as pointed out in refs 13–15. Previous research has already shown that the collision cross section for molecules sticking to a cluster is within experimental uncertainties equal for positively and negatively charged water clusters<sup>16</sup> and is possibly equal for charged and

neutral clusters too.<sup>17,18</sup> Molecular collision cross sections are, however, different from heterogeneous nucleation probabilities, as they do not include the effect of vapor evaporation: Heterogeneous nucleation takes place when the condensation rate of molecules exceeds their evaporation rate.

One source of uncertainty is the procedure which most of the experiments in the past have used to generate ions: production of unipolar ions by a combination of a radioactive source and an electric field, in which neither the size of the ions nor their chemical composition was controlled. Even if the size of the ions was controlled, the unknown chemical composition of the ions causes large uncertainties. The composition of the ions depends on the ion generation method, as well as on different trace gases present in the carrier gas,<sup>19,20</sup> which are often not directly measured. Even if the ions are produced from well-defined starting materials, the chemical composition of the smallest clusters can significantly differ from the bulk material composition for example due to presence of impurities. Thus, precise control over generation and manipulation of the seed ions and particles, as well as knowledge on the properties of the condensing liquid are vital for comprehensive understanding of ion-induced nucleation.<sup>21–23</sup> Moreover, there is almost no research on nucleation onto well-defined sub-3 nm neutral

**Received:** February 22, 2016

**Revised:** March 14, 2016

**Published:** March 15, 2016

seeds, which are comparable to ion-induced nucleation experiments.<sup>4</sup> In this study, we examine the sign preference as a difference in the nucleation probability between charged and neutral seeds. We report experimental observations of heterogeneous nucleation onto size-selected seeds between 0.75 and 3.5 nm in mass equivalent diameter, with three different measured starting materials, three different charging states and three different condensing liquids. The results give new insight on the existence of sign preference during heterogeneous nucleation.

## EXPERIMENTAL METHODS

The test particles were generated with two different methods: glowing wire generator<sup>24,25</sup> and tube furnace.<sup>26</sup> Tungsten oxide particles were generated with a glowing wire generator, in which a resistively heated tungsten wire evaporates tungsten from the surface of the wire. Together with the residue oxygen in the N<sub>2</sub> gas which flushes the wire, the evaporated tungsten vapor forms tungsten oxide particles. Part of the formed particles are natively negatively charged due to the clustering of tungsten oxide with OH<sup>-</sup>,<sup>25</sup> and positively charged particles are similarly formed by clustering with unidentified organic contaminant cations.<sup>23</sup> The tube furnace as a particle generator has been introduced by Scheibel and Porstendörfer.<sup>26</sup> In the furnace, a sample is placed onto a ceramic boat, and the furnace is heated up according to the melting point of the sample. Tetraheptylammonium bromide (THABr) clusters have been previously generated by electrospraying,<sup>27</sup> but singly charged mobility classified clusters have been generated only up to 2.26 nm, which is the electrical mobility equivalent diameter of the positively charged pentamer ( $n = 5$ ).<sup>28</sup> We heated THABr in the furnace in N<sub>2</sub> atmosphere, which allowed formation and size selection of also bigger clusters ( $n > 5$ ) of THABr. The third starting material for the experiments was ammonium sulfate, which was also heated in the furnace.<sup>23</sup> In our experiments the flow rate through the wire generator and the furnace was 10 lpm. Production of particles in high temperatures can easily lead to contaminant species in the formed particles. Therefore, extra care was taken of the cleanliness of the generator surfaces as well as the sample purity grades. To verify the sample composition, a high resolution mass spectrometer was utilized.<sup>29</sup> All experiments were conducted at laboratory temperature of 295 K. The carrier gas was always 5.0 N<sub>2</sub> gas from liquid nitrogen reservoir. The sample gas relative humidity was always close to zero.

The particles generated in the furnace were charged with a radioactive <sup>241</sup>Am source before mobility classification, while the wire generator produces particles that were natively charged. From the charged polydisperse particles a narrow size band (fwhm 4%) was selected with a high resolution Herrmann type differential mobility analyzer (HDMA<sup>28</sup>). The measured mobility was converted to a mass equivalent diameter using eq 17 from Fernandez-Garcia and Fernandez de la Mora<sup>30</sup> and their suggested parameters. The equation includes corrections to ion induced dipole attraction between the charged cluster and polarized neutral carrier gas molecule, and to the diameter of the surrounding gas, which are included in the measured mobility. Downstream of the DMA, the particles were brought to three different nucleation chambers operated with water (TSI 3788<sup>31</sup>), butanol (TSI 3776<sup>32</sup>), or diethylene glycol (DEG; Airmodus A10<sup>33</sup>) and an aerosol electrometer (TSI 3068B). For butanol and diethylene glycol (DEG) the nucleation chambers were operated at the brink of homoge-

neous nucleation to set the vapor supersaturations to comparable points. The nucleation chamber for water was operated at a supersaturation slightly below the limit of homogeneous nucleation due to technical limitations. The TSI 3788 is a laminar type diffusion based ultrafine condensation particle counter (CPC) operated with water as working fluid. The 3788 operates with a 1.5 L per minute (lpm) inlet flow rate, from which 0.6 lpm is extracted and divided as 0.3 lpm sheath flow and 0.3 lpm aerosol flow. The aerosol flow is brought to the center line of the conditioner with the filtered sheath flow around it. This combined flow is cooled in the conditioner and subsequently brought to a heated growth tube, of which walls are wetted with water. Due to the faster diffusion of water vapor compared to heat, supersaturation of water takes place around the center line of the flow, and particle growth occurs. The grown particles are detected optically. The operation temperatures in the experiments were: conditioner 7 °C, growth tube 72 °C, and optics 75 °C. The 3776 utilizes butanol as working fluid. From the inlet flow rate of 1.5 lpm, a flow of 0.3 lpm is extracted, which is divided into a 0.05 lpm capillary flow and a 0.25 lpm sheath flow. The sheath flow is filtered and saturated with butanol. The capillary flow is brought into the center of a cooled condenser with the sheath flow around it. Due to the faster diffusion of heat compared to butanol vapor, supersaturation of butanol takes place in the condenser. The seed particles are grown by butanol and subsequently detected optically. The operation temperatures of the 3776 were: saturator 40 °C, condenser 8 °C, and optics 42 °C. In the A10 the inlet flow rate of 2.5 lpm is mixed with a saturator flow rate of 1 lpm, which is saturated with DEG. The total flow rate of 3.5 lpm is brought to a growth tube in which supersaturation of DEG takes place and particles grow by condensation of DEG. DEG grows the particles up to 90 nm, thus another fine CPC is required to count the particles. The operation temperatures of the A10 were: saturator 82 °C, inlet 35 °C, and growth tube 2 °C.

Figure 1 shows the experimental setup. The experiments were run separately for each of the nucleation chambers to minimize diffusion losses in the sampling line. The diffusion losses in the nucleation chamber inlets were corrected using Gormley and Kennedy.<sup>34</sup> With the HDMA 18 positive and negative voltages were selected, corresponding to diameters

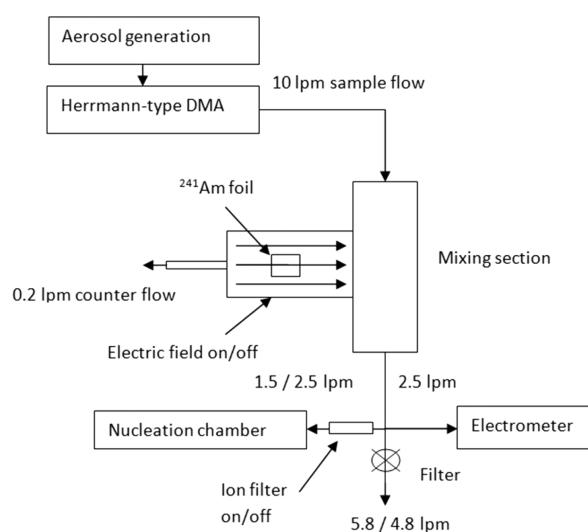


Figure 1. Experimental setup to measure the nucleation probabilities.

from 0.75 to 3.5 nm. The nucleation probability was measured, as  $C_{\text{nucleation chamber}}/C_{\text{electrometer}}$ , where  $C$  is the measured concentration, to obtain the nucleation probability as a function of size for charged particles.

To obtain the nucleation probability for neutral particles, an unipolar neutralizer was placed downstream of the HDMA (described in ref 25), which guides ions from a radioactive  $^{241}\text{Am}$  source against a small counter flow to a mixing chamber, which the sample flow passes through. If the initial sample particles were negatively charged, positively charged ions were guided to the chamber and a fraction of the charged particles were neutralized. Due to no control over the composition of the neutralizing ions, a small uncertainty remains in the composition of the neutralized particles. The uncertainty arises from the unknown composition of the neutralized ions, as well as from the unknown processes taking place when the neutralizing ion collides with the sample particle. The ion can either attach to the particle, replace a molecule from the particle or the particle can even completely fragment due to the collision or chemical reaction with the ion. These processes are probably specific to each ion–particle pair, yielding the uncertainty for the composition of the neutral sample species. However, we observed constant neutralization efficiencies during the experiments with all three sample species. This suggests that there are likely no major issues (such as complete fragmentation of some of the particles) which would prevent the use of the current method. Also, to our knowledge there is no other way to produce size-selected neutral clusters. An on/off ion precipitator was placed downstream of the mixing chamber so that only neutral size selected particles were sampled to the nucleation chamber when the precipitator was on. The electrometer measured the number of the initial charged particles when the neutralizer and ion precipitator were off, and was thus always used as the concentration reference. The number concentration of neutral particles was obtained by measuring the neutralization efficiency of the neutralizer. Two methods were used: measurement of the fraction of neutral particles from the total number of particles after neutralization at sizes, where the nucleation probability can be assumed to be 1. This can be done for example with DEG and tungsten oxide, and by measuring particles larger than 2.5 nm. Another used method was to measure the charged particles with a mass spectrometer with and without the neutralization, and calculate the fraction of the signal intensities. Both methods resulted in fairly constant neutralization efficiencies of 18% in negative and 6.5% in positive polarity. The nucleation probabilities do not reach unity immediately after the steep rise of the curve due to nonuniform supersaturation field inside the nucleation chambers. Also, the chambers are operated at conditions different from the factory settings, which can possibly alter the response of the chambers. However, since the chambers are operated at constant conditions, experiments with varying seed composition are directly comparable. Experiments with varying condensing liquid are comparable, since the nonidealities of the chambers affect mostly the nucleation probabilities close to 0 and unity, not the d50 point, which is the point of our interest.

The nucleation probability was measured for all four charging states: positive, negative, positive neutralized (initially positive sample neutralized with negative ions) and negative neutralized (initially negative sample neutralized with positive ions), for three condensing liquids and for three different seed compositions. This way all the parameters of heterogeneous nucleation can be probed, and the long-standing problem of

sign-preference in heterogeneous nucleation can be directly measured as the difference in the nucleation probability between the charged and neutralized particles.

## RESULTS AND DISCUSSION

**Cluster Composition.** Heating of ammonium sulfate in a furnace in  $\text{N}_2$  atmosphere produced a polydisperse population of clusters with somewhat unexpected compositions. Negatively charged ammonium sulfate particles produced by evaporation–condensation consisted of cluster series with the probable molecular compositions of  $(\text{H}_2\text{S}_2\text{O}_8)_x(\text{NH}_3)_y\text{SO}_4^-$  and  $(\text{H}_2\text{S}_2\text{O}_8)_x(\text{NH}_3)_y\text{HS}_2\text{O}_8^-$ , whereas the positively charged series consisted of  $(\text{H}_2\text{S}_2\text{O}_8)_x(\text{NH}_3)_y\text{H}_2\text{SO}_4^+$  and  $(\text{H}_2\text{S}_2\text{O}_8)_x(\text{NH}_3)_y\text{H}_3\text{S}_2\text{O}_8^+$ . (These elemental compositions can also be written in the form  $(\text{HSO}_4)_a(\text{NH}_3)_b\text{SO}_4^-$  and  $(\text{HSO}_4)_a(\text{NH}_3)_b\text{NH}_4^+$  for negatively and positively charged seeds, respectively, but due to the extremely low probability of multiple highly unstable radicals such as  $\text{HSO}_4$  or  $\text{SO}_4^-$  coexisting in the same cluster without recombining we have chosen not to use this notation.) Thus, the smallest clusters generated with this method were not  $(\text{NH}_4)_2\text{SO}_4$ , which is the composition of the bulk material. There was a major difference in the  $y/x$  ratio of the clusters depending on the size and charging state. For negatively charged clusters the ratio was zero or close to zero for the smallest clusters, meaning that the smallest clusters did not contain, or contained only one ammonia. At 1400 amu the ratio reaches 0.6 (e.g., when  $x = 5$ ,  $y = 2$  for the cluster with highest signal intensity). For positively charged clusters the  $y/x$  ratio was close to 2 throughout the spectrum. Figure 2a,b presents the mass defect plots for positively and negatively charged seed particles formed from heating of ammonium sulfate.

Figure 3a,b shows the mass defect plots for positively and negatively charged tungsten oxide clusters. The negatively charged clusters exhibit a series  $(\text{WO}_3)_x\text{OH}^-$ , while the positively charged clusters exhibit the same  $(\text{WO}_3)_x$  series, but with the charge carrier being an unidentified organic ion.

Positively charged THABr exhibited well separated mobility peaks up to 2.5 nm, which were identified based on their electrical mobility as THABr clusters (Figure 4,  $x$ -axis converted to mass equivalent diameter). Negatively charged THABr did not exhibit as clean mobility spectrum as the positively charged. However, for example the chemical composition of the negatively charged THABr tetramer is the same as of the positively charged trimer, except that it has two Br atoms more. Due to this, the electrical mobility of the negatively charged tetramer is slightly lower than the electrical mobility of the positively charged trimer. This was observed in the mobility spectrum: next to each positively charged mobility peak a less mobile negatively charged peak was observed up to approximately the 9-mer. Since the negatively charged mobility peaks were not as well separated as the positive ones, the negative seeds must have been broadened by some contaminants.

**Nucleation Probabilities.** The experiments revealed several parameters governing the heterogeneous nucleation process. First, with a certain seed composition, DEG started activating particles at smaller sizes than water and butanol (Figure 5, Table 1), which was observed throughout the experiments. For example, the d50 (diameter at which the nucleation probability was 50%) for negatively charged tungsten oxide seeds was 0.65 nm for DEG, 1.46 nm for butanol and 1.76 nm for water. For the three condensing

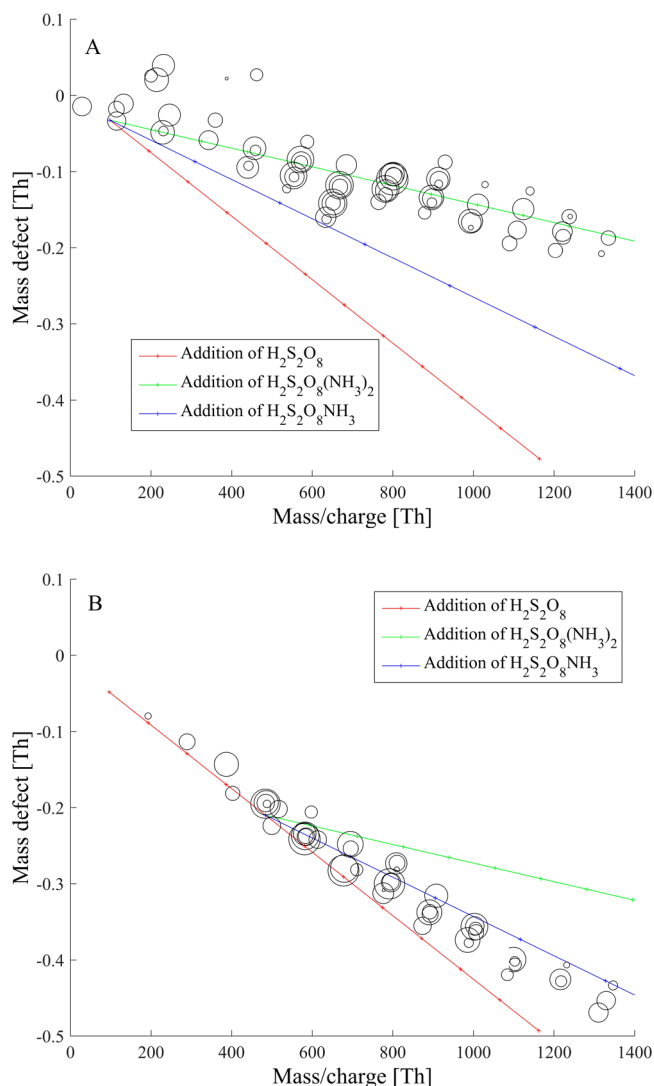


**Figure 2.** Mass defect plots of clusters produced by heating ammonium sulfate. The upper panel (a) corresponds to positively charged clusters, and the lower panel (b) to negatively charged clusters. The circle size corresponds to the signal intensity. The lines show the calculated mass defects as a function of the mass/charge ratio.

liquids, the difference between the smallest and largest  $d_{50}$  for a given seed was observed to be 0.49–1.11 nm.

Second, the difference between minimum and maximum  $d_{50}$  for seeds of different composition was 1.40 nm for water, 1.56 nm for DEG and only 0.78 nm for butanol (Table 1).<sup>21</sup> The differences in  $d_{50}$  between positively and negatively charged seeds of the same starting material can be explained by their different chemical composition. Positively charged tungsten oxide seeds were clustered with, presumably mostly hydrophobic, organic contaminants, while the negatively charged seeds were not. Therefore, smaller negatively charged tungsten oxide seeds were likely more soluble, and thus better activated by the polar solvents, water and DEG. Butanol is neither strongly polar nor strongly nonpolar, and thus showed no or little response to the organic contaminants: the  $d_{50}$  for positively and negatively charged tungsten oxide seeds were equal. The negatively charged seeds produced from heating of ammonium sulfate exhibit a smaller  $d_{50}$  compared to positively charged seeds with all condensing liquids. This may be due to

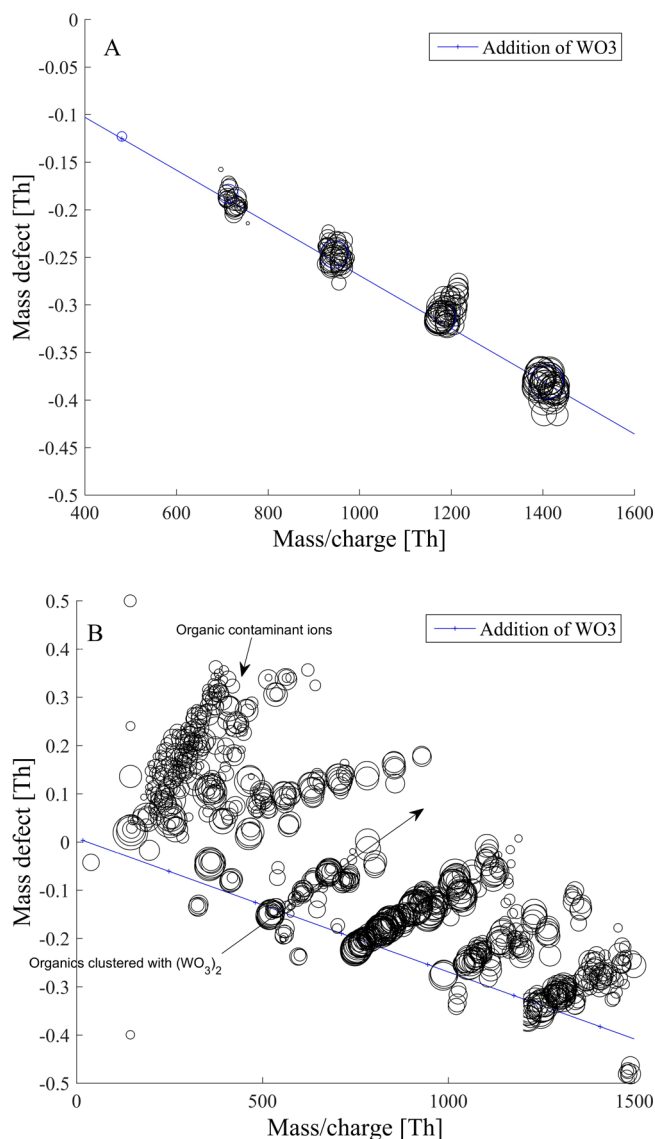


**Figure 3.** Mass defect plot for tungsten oxide seeds. The upper panel (a) corresponds to negatively, and the lower panel (b) to positively, charged clusters. The lines show the calculated mass defects as a function of the mass/charge ratio.

the presence of ammonia in the positively charged clusters. The  $d_{50}$  for positively charged and negatively charged tetraheptylammonium bromide (THABr) were equal for DEG and butanol, but in the case of water the  $d_{50}$  was slightly smaller for negatively charged seeds compared to positively charged seeds. This could be explained by the contaminants observed in the negatively charged clusters of THABr, which could have been water-soluble. Our results clearly demonstrate that small amounts of contaminant molecules, which alter the chemical composition of the clusters, will have an effect on their heterogeneous nucleation probability. Similar results have been obtained by Oberreit et al.,<sup>35</sup> who showed that water uptake of various iodine species strongly depends on the cluster species. If the chemical composition of the clusters is not directly monitored, conclusions on the sign preference cannot be drawn, as other variables besides the electric charge affect the nucleation probability.

The third conclusion from our study was that the  $d_{50}$  was 0–0.50 nm (Table 2) lower for the charged particles compared

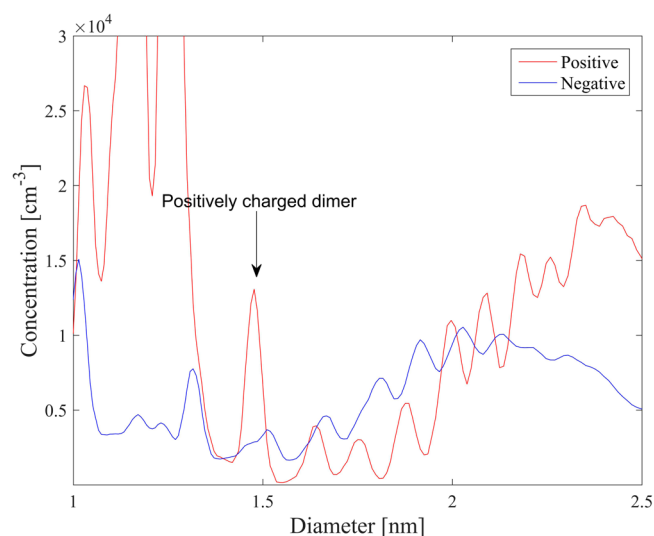


**Figure 4.** Size spectrum for tetraheptylammonium bromide clusters generated with the furnace. Peaks in the spectrum are mobility classified clusters. Red line shows positively charged clusters, blue line negatively charged clusters. Signal below 1.4 nm originates from ions formed in the  $^{241}\text{Am}$  radioactive source.

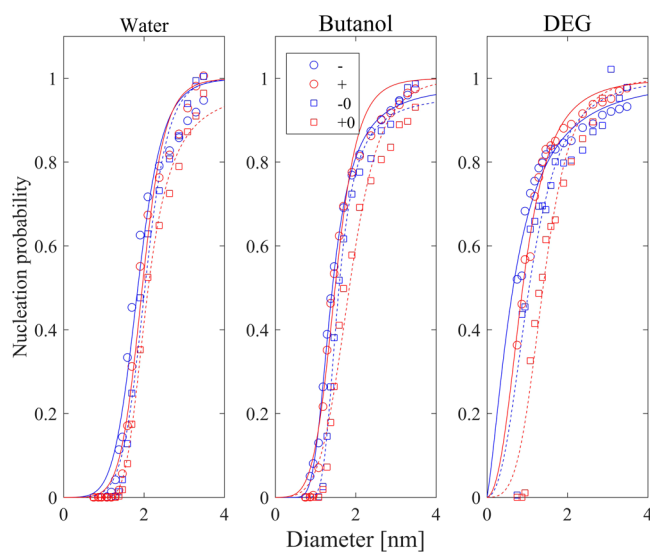


**Figure 5.** Nucleation probability for seeds of tungsten oxide as a function of diameter, for three different condensing liquids (different panels). The charging state of the seeds is indicated with different symbols and colors, lines are fits to the data.  $-0$  and  $+0$  refer to charging state of the seed particles, which were neutralized from originally negatively and positively charged seed particles, respectively.

to the neutral particles of the same chemical composition (charge enhancement). If a sign preference would exist, the difference in the  $d_{50}$  between charged and neutral seeds would have been dependent on the sign (positive or negative), which was not the case. In our experiments no clear preference to positive or negative charge was observed for any of the seeds or liquids, similarly as in ref 36. The experiments did not yield an exact value for the charge enhancement due to the uncertainty in the neutralization process and subsequent uncertainty in the composition of the neutral seed. However, the results show that the relative effect of the charge to the  $d_{50}$  was much smaller than the effect of the seed and vapor composition. This again demonstrates the importance of the seed composition, and the

**Table 1.** All the Measured  $d_{50}$  Diameters for the Condensing Liquid–Seed Material Pairs

material		water	butanol	diethylene glycol
tungsten oxide	–	1.76	1.46	0.65
	0–	1.96	1.65	1.05
	+	1.88	1.43	0.89
ammonium sulfate	0+	2.11	1.84	1.39
	–	1.38	1.69	0.8
	0–	1.52	1.98	1.02
tetraheptylammonium bromide	+	1.44	1.73	0.96
	0+	1.67	2.02	1.12
	–	2.55	1.9	1.66
	0–	2.57	2.09	2.05
	+	2.78	1.9	1.75
	0+	2.7	2.21	2.21

**Table 2.** For a Given Seed Composition, the Table Shows the Difference in the  $d_{50}$  between the Charged and the Neutralized Sample

material		water	butanol	diethylene glycol
tungsten oxide	–	0.2	0.19	0.4
	+	0.23	0.41	0.5
ammonium sulfate	–	0.14	0.29	0.22
	+	0.23	0.29	0.16
tetraheptylammonium bromide	–	0.02	0.19	0.39
	+	–0.08	0.31	0.46

chemistry of the seed-vapor interactions in the research on heterogeneous nucleation process in the size range below 3 nm.

## CONCLUSIONS

We have shown that heterogeneous nucleation of nanoparticles and molecular clusters in supersaturated conditions depends strongly on the condensing vapor and seed particle composition. Solubility effects are the governing factor determining nucleation probabilities in the sub-3 nm size range, the chemical composition of the seed playing an even more important role than the composition of the condensing liquid. Many of the discrepancies in previous experimental results can be accounted for the uncertainty in the seed chemical composition. Even minute amounts of impurities in the clusters changed their heterogeneous nucleation probability compared to a pure cluster. Generally, negatively charged oxidized or acidic particles are less contaminated by organic or other molecules than positively charged particles, causing heterogeneous nucleation of polar vapors to occur more probably on negatively charged particles. In other seed-vapor systems, the apparent sign preference can be also the opposite.<sup>6</sup>

The observed nucleation probabilities for neutral particles revealed that heterogeneous nucleation does not clearly favor positively or negatively charged particles. Earlier research on sign preference has compared only the difference between positively and negatively charged particles (except in ref 4), often without direct information on ion size or chemical composition. This has led to a bias due to the different chemical composition of the positively charged and negatively charged particles, which plays a significant role in heterogeneous nucleation, and thus explains the diverse, contradicting conclusions on the sign-preference. We conclude that no systematic sign preference exists for any of the used condensing

liquids and seeds, but cannot rule out its existence in any specific single system. In the future, more precise control over seed properties, especially the controlled generation of electrically neutral size-selected sub-3 nm seeds, together with high resolution mass and mobility analysis, with possibly mass spectrometric methods to detect the first steps, will provide further insights into heterogeneous nucleation.

## AUTHOR INFORMATION

### Corresponding Author

\*Phone +358503185096. E-mail: [juha.kangasluoma@helsinki.fi](mailto:juha.kangasluoma@helsinki.fi).

### Notes

The authors declare no competing financial interest.

## ACKNOWLEDGMENTS

This work was partly funded by European Research Council (ATMNUCLE, 227463, MOCAPAF,257360), Academy of Finland (Center of Excellence Program Projects 1118615 and 139656, Research Fellow Project 1266388), Nordic Center for Excellence (CRAICC), European Commission seventh Framework program (ACTRIS, Contract No. 262254; ACTRIS2 Contract No. 654109; PEGASOS, Contract No. 265148), Office of Science (BER), the European Union's Horizon 2020 research and innovation program under the Marie Skłodowska-Curie Grant Agreement No. 656994, and U.S. Department of Energy (The Biogenic Aerosols – Effects of Clouds and Climate, BAEC).

## REFERENCES

- (1) Wilson, C. T. R. On the Condensation Nuclei Produced in Gases by the Action of Rontgen Rays, Uranium Rays, Ultra-Violet Light, and Other Agents. *Philos. Trans. R. Soc., A* **1899**, 192, 403–453.
- (2) Kirkby, J.; Curtius, J.; Almeida, J.; Dunne, E.; Duplissy, J.; Ehrhart, S.; Franchin, A.; Gagne, S.; Ickes, L.; Kurten, A.; et al. Role of Sulphuric Acid, Ammonia and Galactic Cosmic Rays in Atmospheric Aerosol Nucleation. *Nature* **2011**, 476, 429–433.
- (3) Rusanov, A. I.; Kuni, F. M. Reformulation of the Thermodynamic Theory of Nucleation on Charged-Particles. *J. Colloid Interface Sci.* **1984**, 100, 264–277.
- (4) Winkler, P. M.; Steiner, G.; Vrtala, A.; Vehkamäki, H.; Noppel, M.; Lehtinen, K. E. J.; Reischl, G. P.; Wagner, P. E.; Kulmala, M. Heterogeneous Nucleation Experiments Bridging the Scale from Molecular Ion Clusters to Nanoparticles. *Science* **2008**, 319, 1374–1377.
- (5) Nadykto, A. B.; Yu, F. Q.; Herb, J. Towards Understanding the Sign Preference in Binary Atmospheric Nucleation. *Phys. Chem. Chem. Phys.* **2008**, 10, 7073–7078.
- (6) Adachi, M.; Okuyama, K.; Seinfeld, J. H. Experimental Studies of Ion-Induced Nucleation. *J. Aerosol Sci.* **1992**, 23, 327–337.
- (7) Seto, T.; Okuyama, K.; de Juan, L.; Fernández de la Mora, J. Condensation of Supersaturated Vapors on Monovalent and Divalent Ions on Varying Size. *J. Chem. Phys.* **1997**, 107, 1576–1585.
- (8) Okuyama, K.; Adachi, M.; Shinagawa, H.; Shi, G.; Seinfeld, J. H. Experimental-Study of Nucleation on Ions with Dbp Vapor. *J. Aerosol Sci.* **1991**, 22, S85–S88.
- (9) Kane, D.; Daly, G. M.; Elshall, M. S. Condensation of Supersaturated Vapors on Benzene Ions Generated by Resonant 2-Photon Ionization - a New Technique for Ion Nucleation. *J. Phys. Chem.* **1995**, 99, 7867–7870.
- (10) Katz, J. L.; Fisk, J. A.; Chakarov, V. M. Condensation of a Supersaturated Vapor 0.9. Nucleation on Ions. *J. Chem. Phys.* **1994**, 101, 2309–2318.
- (11) Oh, K. J.; Gao, G. T.; Zeng, X. C. Nucleation of Water and Methanol Droplets on Cations and Anions: The Sign Preference. *Phys. Rev. Lett.* **2001**, 86, 5080–5083.
- (12) Rabeony, H.; Mirabel, P. Experimental-Study of Vapor Nucleation on Ions. *J. Phys. Chem.* **1987**, 91, 1815–1818.
- (13) Nadykto, A. B.; Al Natsheh, A.; Yu, F.; Mikkelsen, K. V.; Ruuskanen, J. Quantum Nature of the Sign Preference in Ion-Induced Nucleation. *Phys. Rev. Lett.* **2006**, 96, 125701.
- (14) Kathmann, S. M.; Schenter, G. K.; Garrett, B. C. Ion-Induced Nucleation: The Importance of Chemistry. *Phys. Rev. Lett.* **2005**, 94, 116104.
- (15) Castleman, A. W.; Tang, I. N. Role of Small Clusters in Nucleation About Ions. *J. Chem. Phys.* **1972**, 57, 3629–3638.
- (16) Zamith, S.; de Tournadre, G.; Labastie, P.; L'Hermite, J. M. Attachment Cross-Sections of Protonated and Deprotonated Water Clusters. *J. Chem. Phys.* **2013**, 138, 03430110.1063/1.4775401
- (17) Lengyel, J.; Pysanenko, A.; Poterya, V.; Slavíček, P.; Fárník, M.; Kočíšek, J.; Fedor, J. Irregular Shapes of Water Clusters Generated in Supersonic Expansions. *Phys. Rev. Lett.* **2014**, 112, 10.1103/PhysRevLett.112.113401
- (18) Braud, I.; Boulon, J.; Zamith, S.; L'Hermite, J. M. Attachment of Water and Alcohol Molecules onto Water and Alcohol Clusters. *J. Phys. Chem. A* **2015**, 119, 6017–6023.
- (19) Steiner, G.; Reischl, G. P. The Effect of Carrier Gas Contaminants on the Charging Probability of Aerosols under Bipolar Charging Conditions. *J. Aerosol Sci.* **2012**, 54, 21–31.
- (20) Steiner, G.; Jokinen, T.; Junninen, H.; Sipilä, M.; Petäjä, T.; Worsnop, D.; Reischl, G. P.; Kulmala, M. High-Resolution Mobility and Mass Spectrometry of Negative Ions Produced in a Am-241 Aerosol Charger. *Aerosol Sci. Technol.* **2014**, 48, 261–270.
- (21) Kangasluoma, J.; Kuang, C.; Wimmer, D.; Rissanen, M. P.; Lehtipalo, K.; Ehn, M.; Worsnop, D. R.; Wang, J.; Kulmala, M.; Petäjä, T. Sub-3 Nm Particle Size and Composition Dependent Response of a Nano-Cpc Battery. *Atmos. Meas. Tech.* **2014**, 7, 689–700.
- (22) Winkler, P. M.; Vrtala, A.; Steiner, G.; Wimmer, D.; Vehkamäki, H.; Lehtinen, K. E. J.; Reischl, G. P.; Kulmala, M.; Wagner, P. E. Quantitative Characterization of Critical Nanoclusters Nucleated on Large Single Molecules. *Phys. Rev. Lett.* **2012**, 108, 10.1103/PhysRevLett.108.085701
- (23) Kangasluoma, J.; Junninen, H.; Lehtipalo, K.; Mikkilä, J.; Vanhanen, J.; Attoui, M.; Sipilä, M.; Worsnop, D.; Kulmala, M.; Petäjä, T. Remarks on Ion Generation for Cpc Detection Efficiency Studies in Sub-3-Nm Size Range. *Aerosol Sci. Technol.* **2013**, 47, 556–563.
- (24) Peineke, C.; Attoui, M.; Robles, R.; Reber, A. C.; Khanna, S. N.; Schmidt-Ott, A. Production of Equal Sized Atomic Clusters by a Hot Wire. *J. Aerosol Sci.* **2009**, 40, 423–430.
- (25) Kangasluoma, J.; Attoui, M.; Junninen, H.; Lehtipalo, K.; Samodurov, A.; Korhonen, F.; Sarnela, N.; Schmidt-Ott, A.; Worsnop, D.; Kulmala, M.; et al. Sizing of Neutral Sub 3 Nm Tungsten Oxide Clusters Using Airmodus Particle Size Magnifier. *J. Aerosol Sci.* **2015**, 87, 53–62.
- (26) Scheibel, H. G.; Porstendörfer, J. Generation of Monodisperse Ag- and NaCl- Aerosols with Particle Diameters between 2 and 300 Nm. *J. Aerosol Sci.* **1983**, 14, 113–126.
- (27) Ude, S.; Fernández de la Mora, J. Molecular Monodisperse Mobility and Mass Standards from Electrosprays of Tetra-Alkyl Ammonium Halides. *J. Aerosol Sci.* **2005**, 36, 1224–1237.
- (28) Kangasluoma, J.; Attoui, M.; Korhonen, F.; Ahonen, L.; Siivola, E.; Petäjä, T. Characterization of a Herrmann Type High Resolution Differential Mobility Analyzer. *Aerosol Sci. Technol.* **2016**, 50, 222–229.
- (29) Junninen, H.; Ehn, M.; Petäjä, T.; Luosujärvi, L.; Kotiaho, T.; Kostianen, R.; Rohner, U.; Gonin, M.; Fuhrer, K.; Kulmala, M.; et al. A High-Resolution Mass Spectrometer to Measure Atmospheric Ion Composition. *Atmos. Meas. Tech.* **2010**, 3, 1039–1053.
- (30) Fernandez-Garcia, J.; Fernandez de la Mora, J. Measuring the Effect of Ion-Induced Drift-Gas Polarization on the Electrical Mobilities of Multiply-Charged Ionic Liquid Nanodrops in Air. *J. Am. Soc. Mass Spectrom.* **2013**, 24, 1872–1889.
- (31) Iida, K.; Stolzenburg, M. R.; McMurry, P. H.; Smith, J. N.; Quant, F. R.; Oberreit, D. R.; Keady, P. B.; Eiguren-Fernandez, A.; Lewis, G. S.; Kreisberg, N. M.; et al. An Ultrafine, Water-Based

Condensation Particle Counter and Its Evaluation under Field Conditions. *Aerosol Sci. Technol.* **2008**, *42*, 862–871.

(32) Stolzenburg, M. R.; McMurry, P. H. An Ultrafine Aerosol Condensation Nucleus Counter. *Aerosol Sci. Technol.* **1991**, *14*, 48–65.

(33) Vanhanen, J.; Mikkilä, J.; Lehtipalo, K.; Sipilä, M.; Manninen, H. E.; Siivola, E.; Petäjä, T.; Kulmala, M. Particle Size Magnifier for Nano-Cn Detection. *Aerosol Sci. Technol.* **2011**, *45*, 533–542.

(34) Gormley, P. G.; Kennedy, M. Diffusion from a Stream Flowing through a Cylindrical Tube. *Proc. R. Irish Acad.* **1949**, *52*, 163–169.

(35) Oberreit, D.; Rawat, V. K.; Larriba-Andaluz, C.; Ouyang, H.; McMurry, P. H.; Hogan, C. J. Analysis of Heterogeneous Water Vapor Uptake by Metal Iodide Cluster Ions Via Differential Mobility Analysis-Mass Spectrometry. *J. Chem. Phys.* **2015**, *143*, 104204.

(36) Abdelsayed, V.; El-Shall, M. S. Direct Observation of Metal Nanoparticles as Heterogeneous Nuclei for the Condensation of Supersaturated Organic Vapors: Nucleation of Size-Selected Aluminum Nanoparticles in Acetonitrile and N-Hexane Vapors. *J. Chem. Phys.* **2014**, *141*, 054710.